International Journal of Electrical and Computer Engineering (IJECE)
Vol. 10, No. 1, February 2020, pp. 816~827
ISSN: 2088-8708, DOI: 10.11591/ijece.v10i1.pp816-827

Automated fundus image quality assessment and segmentation of optic disc using convolutional neural networks

Bhargav Bhatkalkar[1], Abhishek Joshi[2], Srikanth Prabhu[3], Sulatha Bhandary[4]
[1,3]Department of Computer science and Engineering, Manipal Institute of Technology, Manipal Academy of Higher Education, India
[2]Department of Electronics and Communication Engineering, Manipal Institute of Technology, Manipal Academy of Higher Education, India
[4]Department of Ophthalmology, Kasturba Medical College, Manipal Academy of Higher Education, India

Article Info

Article history:

Received May 4, 2019
Revised Oct 15, 2019
Accepted Oct 8, 2019

Keywords:

Convolutional neural network
Foreground object
GrabCut algorithm
Image quality assessment
Optic disc

ABSTRACT

An automated fundus image analysis is used as a tool for the diagnosis of common retinal diseases. A good quality fundus image results in better diagnosis and hence discarding the degraded fundus images at the time of screening itself provides an opportunity to retake the adequate fundus photographs, which save both time and resources. In this paper, we propose a novel fundus image quality assessment (IQA) model using the convolutional neural network (CNN) based on the quality of optic disc (OD) visibility. We localize the OD by transfer learning with Inception v-3 model. Precise segmentation of OD is done using the GrabCut algorithm. Contour operations are applied to the segmented OD to approximate it to the nearest circle for finding its center and diameter. For training the model, we are using the publicly available fundus databases and a private hospital database. We have attained excellent classification accuracy for fundus IQA on DRIVE, CHASE-DB, and HRF databases. For the OD segmentation, we have experimented our method on DRINS-DB, DRISHTI-GS, and RIM-ONE v.3 databases and compared the results with existing state-of-the-art methods. Our proposed method outperforms existing methods for OD segmentation on Jaccard index and F-score metrics.

Corresponding Author:

Bhargav Bhatkalkar, Srikanth Prabhu,
Department of Computer Science and Engineering,
Manipal Institute of Technology,
Manipal Academy of Higher Education,
Manipal, 576104, India.
Email: bhargav.jb@manipal.edu, abhist20@gmail.com, srikanth.prabhu@manipal.edu

1. INTRODUCTION

Retinal imaging is a non-invasive technique of taking pictures of the retinal layer. The ophthalmologists perceive the majority of the eye diseases by analyzing the retinal images. Computer-aided automated diagnosis is used to identify retinal diseases with high precision, and to classify them into different stages. Based on the severity and nature of the retinal disease detected, treatment can be prioritized. Glaucoma, which is the second major cause of blindness all over the world [1], is expected to increase by another 20 million by the end of 2020 [2, 3]. Macular degeneration is another disease which is found to cause the majority of blindness commonly among old aged people [4]. Disease like the macular hole is very difficult to recover from if detected in its later stages. Therefore, identifying these diseases in their early stages is very important to avoid the loss of vision.

Color fundus image provides the visual details of essential anatomical components of the retina like an optic disc (OD), macula, optic nerve head, retinal veins, retinal arteries, etc. as shown in Figure 1.

Ophthalmologists can efficiently identify common ocular diseases like glaucoma, macular hole, diabetic retinopathy, and macular degeneration in fundus images. In a color fundus image, the OD appears as a bright elliptical region having two distinct zones, namely, the optic cup and optic disc. The localization and segmentation of OD play a vital role in the correct localization of other anatomical structures like macula and optic nerve head, which is essential in the detection of the progress of diseases like macular hole and glaucoma into their later stages [5, 6]. The macula is a pigmented area situated near the center of the retina. The center of the macula is known as the fovea, which is responsible for our central vision required to perform day to day activities. The center and the diameter of OD are used to establish polar fundus coordinates (PFC) centered on fovea [7] as shown in Figure 2. PFC helps in grading the severity of macular diseases based on their proximity to the center of the macula.

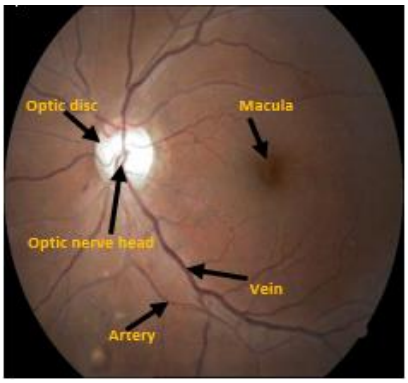

Figure 1. Anatomical statures of a human eye

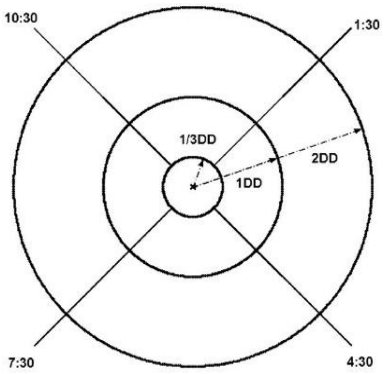

Figure 2. Polar fundus coordinates; DD (disc diameter)

Retinal diseases bring in the pathological changes in the anatomy of the retina. Diseases like optic disc edema, optic disc hemorrhages, and glaucoma sometimes make the segmentation of OD very hard [8]. Also, in many cases, the quality of fundus images is not good enough to detect the OD precisely. We can improve the efficiency and effectiveness of an automated diagnosis method by discarding the degraded quality images at the time of retinal screening and hence considering only the good quality images for processing [9]**.** There are different methods available for the image quality assessments, but with the recent advancements in deep learning, very efficient fundus image classification network can be designed [10].

We select a region of interest (ROI) in an image to focus only on a small area in the entire image. Selecting an ROI in an image has become a straightforward task with the aid of deep neural networks. We train the network with a pair of image and label representing the ROI. An expert in the specific field selects the coordinates for the label. Upon training, the network predicts the correct possible label for any input image.

An ROI in a fundus image contains the objects of paramount importance like optic disc and macula. These objects are the anatomical components of the retina. The region inside the ROI is called the foreground, and the region outside the ROI is known as background. Objects of interest lie inside the foreground region, and precise segmentation of these objects is very crucial in the detection and classification of retinal diseases. After the foreground objects are segmented, contours can be plotted for these objects to approximate their diameter, center, area, shape, perimeter, etc.

In this paper, we present a novel deep neural network to classify the fundus images based on the quality of OD. We use transfer learning with Inception-v3 [11] model to select the ROI containing OD. GrabCut algorithm [12] is used to precisely segment the OD as a foreground object in the ROI, and finally, contour operations are used to get the center and diameter of OD. We have implemented the proposed method in Python 3.6.8. Using Tensorflow 1.14.0 library.

2. RELATED WORK

An accurate retinal disease diagnosis solely depends on the quality of the fundus image captured. In recent years, there has been good amount of work done in fundus IQA using Convolutional Neural Networks (CNN). The first CNN based fundus IQA algorithm was proposed in the paper [13]. The method leverages the underlying principles of the human visual system (HVS) in the design of a novel CNN which learns all the necessary features required for grading/degrading an image without the use of hand-crafted

features in the image. The work proposed in [14] defined a unique way of fusing the features obtained by saliency map [15] with the features extracted from a CNN network to assess the quality of the fundus image. A total of 3000 and 2200 fundus images were used for training and testing the network, respectively. The authors have used SVM classifier to classify the fundus images into either good or bad qualities instead of the traditional sigmoid function. The grading of fundus images in the context of diabetic retinopathy was proposed in [9] using a deep CNN with a total of 7000 color fundus images used for the experiment. The classification of fundus images for retinopathy of prematurity (ROP) is proposed in the paper [10]. The authors have used 6043 color fundus images of premature infants to train and validate their network.

Application of CNN has become a standard approach for the OD segmentation in recent years. Authors of paper [16] have used transfer learning with VGG-16 network to segment the OD with high accuracy. They have used dice score and boundary error evaluation metrics for comparing the result of their network. A modified U-net architecture is proposed in [17] for the detection of glaucoma by segmentation of both OD and optic cup (OC). The method requires the cropping of the OD region of interest and passing it to the modified U-Net through CLAHE step. The trainable parameters in the network are very less, and the network is very much light-weighted compared to the original U-Net model. The recent work proposed in M-Net [18] jointly segments OD and OC using a four-layered architecture. The first layer produces an image pyramid to improve the accuracy of segmentation, and the second layer is a modified U-Net which performs the segmentation of OD and OC. The third layer is a slide-output layer which acts as a classifier. The final fourth layer assigns each output instance to multiple binary labels.

The region of interest (ROI) marks the boundary between foreground and background regions in an image. The objects present in the foreground region are the subjects of interest. The precise segmentation of foreground objects defines the accuracy of any segmentation algorithm. GrabCut [19] is a robust algorithm for segmenting the foreground objects from an ROI. The user will select a rectangular ROI around the objects to mark the boundary between the foreground and the background. It is an iterative algorithm designed by combining GraphCut algorithm [20, 21] and statistical models of color space. In paper [22], the authors have proposed a segmentation model by combining GrabCut with linear multiscale smoothing method. In the method, when a Gaussian kernel is run iteratively through an ROI, multiple multi-scale smoothing components, each representing different levels of image information is produced. The GrabCut algorithm is then applied to segment each component independently. The authors in paper [23] have proposed a technique to speedup GrabCut by separating its segmentation step in two hierarchical steps. They propose a two-step procedure where first they repeatedly apply segmentation on a low-resolution version of the original image till it converges. In the second step, the parameters of first segmentation are used to initialize the second round of segmentation on the original image. Since the segmentation on low-resolution images happens fast compared to the high-resolution images, the overall speed using this two-step approach is fast compared to the traditional GrabCut algorithm.

3. PROPOSED METHOD

The method uses a novel classification network for classifying the fundus images into either good quality or bad quality based on the visibility of optic disc. Only the good quality images are selected, and their quality is further improved using image enhancement techniques. We are using transfer learning to select an ROI containing the optic disc in enhanced images. The GrabCut algorithm is then used to segment the optic disc as a foreground object in the ROI. Finally, the diameter of the optic disc is determined by plotting the contour to the foreground object and approximating it to a circle. Figure 3 lists all the steps in the proposed method.

3.1. Image quality assessment

We propose a novel CNN for assessing the quality of retinal images based on the quality of optic disc in the images. Since the diameter of the optic disc plays a vital role in the determination of foveal coordinate system, as shown in Figure 2, it is very essential to compute it as accurately as possible. If the optic disc is not clearly visible or if the optic disc is not completely visible in the retinal image, finding its precise diameter may not be possible. The network classifies the fundus images into good quality if the optic disc is clearly and completely visible in the retinal image or else the image is classified as bad quality, and it is discarded.

The image quality assessment network is shown in Figure 4. The input for the classifier is a $224 * 224 * 3$ fundus image, and the output is a single node that gives the probability of input image being good quality or bad quality. Table 1 shows the databases and the number of images used in them for training the classification network. A few examples of fundus images used for training the network is shown in Figure 5. The images in Figure 5(a)-(d) are the good quality images because the optic disc is clearly and

completely visible. The images in Figure 5(e)-(h) are bad quality fundus images. In Figure 5(e), there is no optic disc present. In Figure 5 (f)-(g), only the partial optic disc is visible. In Figure 5(h), the optic disc is not clearly distinguishable due to the pathological change as a result of some retinal disease.

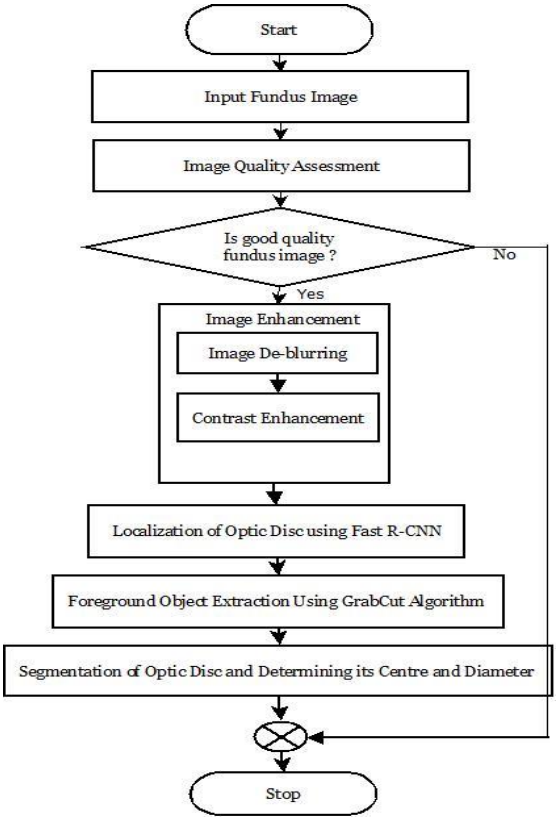

Figure 3. Proposed method

Figure 4. Fundus image quality assessment network

Table 1. Databases used for training classification network

Database	Number of good quality images	Number of bad quality images
STARE	172	225
DRIMDB	106	89
ONHSD	92	7
KMC	213	114
Total:	*583*	*435*

In the classification network, after every $3 * 3$ padded convolutions with a stride of 1, a batch normalization layer is added to speed-up the model learning rate and to minimize the problem of 'Internal Covariate Shift. The use of batch normalization layers in the model helps in faster convergence [24]. A Leaky ReLU activation function with α=0.1 is used after the batch normalization as given in (1). After the activation, a max-pooling layer of $2 * 2$ with a stride of 1 is used for down-sampling the images.

$$Leaky\ ReLU = f(x) = \begin{cases} x, x > 0 \\ \alpha * x, x \leq 0 \end{cases} \quad (1)$$

After the last batch normalization layer, a Global Average Pooling (GAP) layer is used to reduce the number of trainable parameters in the network instead of flattening into a $14 * 14 * 128$ vector. A GAP layer would produce only 128 nodes before the final node, in contrast to 25088 nodes if a fully-connected dense layer were used. Between the GAP layer and the output layer, Dropout layer is introduced with a probability of 0.5 for reducing the overfitting while training [25]. Dropout regularization is used to make the model generalize better by preventing overfitting, and it makes the model highly robust. The sigmoid function is used as an activation function for the output node.

(a) (b) (c) (d)

(e) (f) (g) (h0

Figure 5. Examples of training images;
(a)-(d) Good quality fundus images; (e)-(h) Bad quality fundus images

3.2. Image enhancement

There are three different color channels available in the RGB images, namely red channel, green channel, and blue channel. We use the green channel of the given fundus image for extracting the optic disc as the critical anatomical structures of the retina like the optic disc, macula, optic nerves are more clearly visible in the green channel compared to other two channels. The input fundus image is subjected to two image enhancement techniques, namely de-blurring and contrast enhancement.

We use iterative Lucy–Richardson *deconvolution* algorithm [26, 27] for de-blurring the images, which reduce the intensity gradient feature of the image pixels. We consider two-dimensional green channel images whose brightness is represented by a function defined on a rectangular region $\Omega \in \mathbb{R}^2$. Let the contaminated image with noise and blur be represented by the function b^{δ}. Let the function $\hat{x}$ represent the unknown noise and, blur free image that we aim to recover. We assume that the functions b^{δ} and $\hat{x}$ are related to each other by the degradation model given in the (2).

$$b^{\delta}(s) = \int_{\Omega} h(s,t)\, \hat{x}(t)\, dt + \eta\delta_{(s),s\in\Omega} \quad (2)$$

Where, $\eta\delta$ is the noise present in the contaminated image b^{δ}. The kernel h models the blurring in the image as given by the (3).

$$h(s,t) = h(t,s) = k_{(s-t),s,t} \in \Omega \quad (3)$$

From the given (2) and (3), the Lucy–Richardson method for $\Omega \in \mathbb{R}^p$ with $p > 1$, where p is an integer is defined in the (4).

$$x_{r+1}(u) = x_r(u) \int_{\mathbb{R}^P} \frac{k(S-u)b^{\delta}(S)}{\int_{\mathbb{R}^P} k(S-t)x_r(t)\,dt} ds, u \in \mathbb{R}^P, r = 0,1,., \quad (4)$$

The contrast is an essential visual property of any digital image. Contrast enhancement is a commonly used technique for improving the quality of an image. The proposed method uses Contrast Limited Adaptive Histogram Equalization (CLAHE) [28, 29] technique for enhancing the overall contrast of the image. Let the variable r represents the gray-level of an image to be enhanced, T is the transformation function. The transformed value s is given by (5).

$$s = T(r) = 0^{\int_{P_r}^{\gamma}(\omega)\,dw} \quad (5)$$

If pr and ps represent the probability density function of r and s respectively, then ps can be obtained by applying a simple formula as given in the (6).

$$Ps\,(s) = Pr(r)\,\left|\frac{dr}{ds}\right| \quad (6)$$

Given a transformation function T(r), we can get Pr so that $Ps\,(s)$ follows almost uniform distribution, which results in histogram equalized image. Figure 6 shows the results of image enhancement.

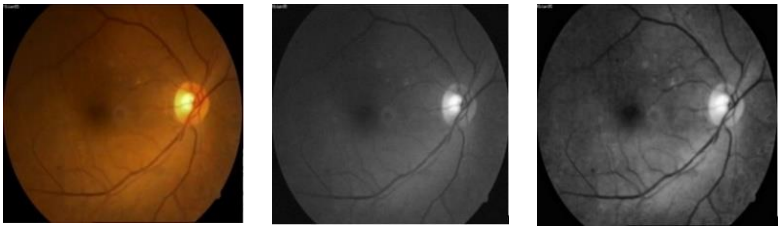

(a) (b) (c)

Figure 6. Image enhancement;
(a) Input image; (b) De-blurred green channel image; (c) Contrast-enhanced image

3.3. Localization of optic disc using Inception-v3 model

We are using Inception-v3 model to localize the optic disc in the fundus image. The model is trained on good quality fundus images of datasets listed in Table 1. For training the network, we give the retinal image and the four coordinates of the bounding box comprising the optic disc in it as its label. The bounding box is manually selected, and the four coordinates are then extracted. Figure 7 shows sample examples of bounding boxes labeled for training. For an enhanced fundus image as input, the network outputs a predicted ROI localizing the optic, as shown in Figure 8.

(a) (b) (c) (d)

Figure 7. Training Inception-v3; (a-d) Bounding box labels

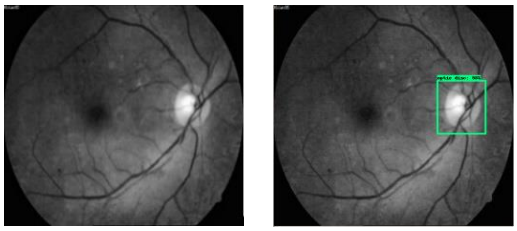

(a) (b)

Figure 8. Inception-v3 output;
(a) Input image; (b) Predicted ROI localizing the optic disc and its prediction score displayed

3.4. Segmentation of optic disc using GrabCut algorithm

The ROI selected in the previous step marks the foreground and background regions for the GrabCut algorithm to detect the foreground object. Following are the steps employed by the GrabCut [30] algorithm to segment the foreground object, which is the optic disc:

a. Initially, everything outside the ROI is considered as sure known background, and everything inside the ROI is taken as unknown.
b. The initial image segmentation is performed by tentatively placing all unknown pixels in the foreground class and all known background pixels in the background class.
c. Gaussian Mixture Models (GMM) are created for the initial foreground and background classes.
d. Each pixel in the foreground class is assigned to the most likely Gaussian component in the foreground GMM. Same is done with the background pixels but with the background GMM.
e. From the pixel sets created in the previous *step 4*, new GMMs are learned, and old GMMs are discarded.
f. Now a graph is built, and the Graph Cut algorithm is used to find the new tentative classification of foreground and background pixels.
g. The *steps 4* to *6* repeated until the classification process converges. The outcome of this step is the extraction of the foreground object in the given ROI, which is the OD.

The ROI input to the GrabCut algorithm and its output as the segmented optic disc is shown in Figure 9.

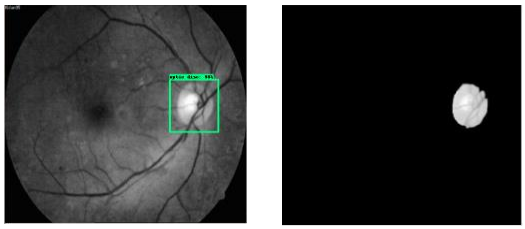

(a) (a)

Figure 9. GrabCut algorithm output. (a) Input image with ROI; (b) Optic disc segmentation

3.5. Determining optic disc diameter

For the optic disc segmented in the previous step, a contour is drawn and then approximated to the nearest possible circle. Approximation to a circle is performed to compute the center and diameter of OD. The diameter of the optic disc is found in terms of pixels using Root Mean Square (RMS) method of approximation as given by the (7). We map the coordinates of the contours to the input color fundus image to show the segmented optic disc. All the steps involved in contour manipulation and circle approximation are shown in Figure 10.

$$\lim_{T \to 2} \sqrt{\frac{1}{T} \sum_{i=1}^{2} (Di)^2} \quad (7)$$

Where D1 is the area of optic disc and D2 is the perimeter of the optic disc.

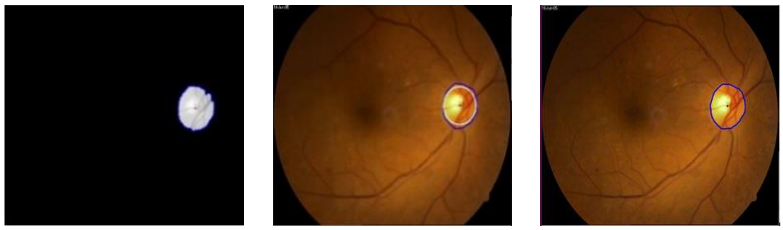

(a) (b) (c)

Figure 10. Finding the diameter of the optic disc; Black dot represents the center of optic disc; (a) Contour for foreground object (b) Contour approximated to circle (c) Segmented optic disc in the original input image

4. RESULTS AND ANALYSIS

The confusion matrix parameters are used to assess the performance of image quality assessment network on three retinal test databases. These parameter values are given in Table 2. The parameters are defined as follows:

- *True-Positive (TP):* Fundus image quality is good, and the network classified it as good quality image.
- *True-Negative (TN):* Fundus image quality is bad, and the network classifies it as bad quality image.
- *False-Positive (FP):* Fundus image quality is bad, but the network classifies it as good quality image.
- *False-Negative (FN):* Fundus image quality is good, but the network classifies it as bad quality image.

Table 2. Confusion matrix parameters

Database Name	Number of Images (Good quality + Bad quality)	TP	TN	FP	FN
DRIVE	40 (37+3)	37	3	0	0
CHASE-DB	28 (22+6)	22	5	1	0
HRF	45 (42+3)	42	2	1	0

Table 3 lists the accuracy of classification network for the three fundus test databases with respect to four evaluation metrics, namely Recall, Precision, Accuracy, and Misclassified Portion (MP).

$$Recall = \frac{TP}{TP+FN}; Precision = \frac{TP}{TP+FP}; Accuracy = \frac{TP+TN}{TP+FP+TN+FN}; MP = \frac{FP+FN}{TP+FP+TN+FN}$$

Table 3. Classification accuracy

Database Name	Recall	Accuracy	Precision	MP
DRIVE	100%	100%	100%	0%
CHASE-DB	100%	96.4%	95.6%	3.6%
HRF	100%	97.8%	97.7%	2.2%

The proposed method achieved a success rate of 98.72%, 99.21% and 96.43% on DRIONS-DB database, DRISTI-GS database, and RIM-ONE database respectively for the optic disc segmentation. The evaluation metric used is average Intersection Over Union (IOU) [31], and F-Score is given by the (8) and (9) respectively. The segmentation performance of the proposed method with other existing methods is summarized in Table 4. The segmentation of optic disc in fundus images of different databases is shown in Figure 11.

$$J(A,B) = \frac{|A \cap B|}{|A \cap B|} \quad (8)$$

Where A and B are binary vectors representing the ground truth and predicted mask, respectively.

$$F\text{-}score = 2.\frac{Precision * Recall}{Precision + Recall} \quad (9)$$

Table 4. Segmentation accuracy in terms of Jaccard index (J) and F-score (F). "-" indicates that the result not reported

Author	Type	DRIONS-DB	DRISHTI-GS	RIM-ONE v.3
Maninis et al. [16]	J	89.0	-	89.0
Sevastopolsky [17]	J	89.0	75.0	89.0
Aquino et al. [32]	F	-	93.2	90.1
	J		86.1	84.2
Cheng et al. [33]	F	-	89.2	89.2
	J		82.9	82.9
Joshi et al. [34]	F	-	96.0	93.1
	J		90.1	88.0
Zilly et al. [35]	F	-	97.3	94.2
	J		91.4	89.0
Our approach	F	93.4	93.7	94.8
	J	91.2	93.2	91.5

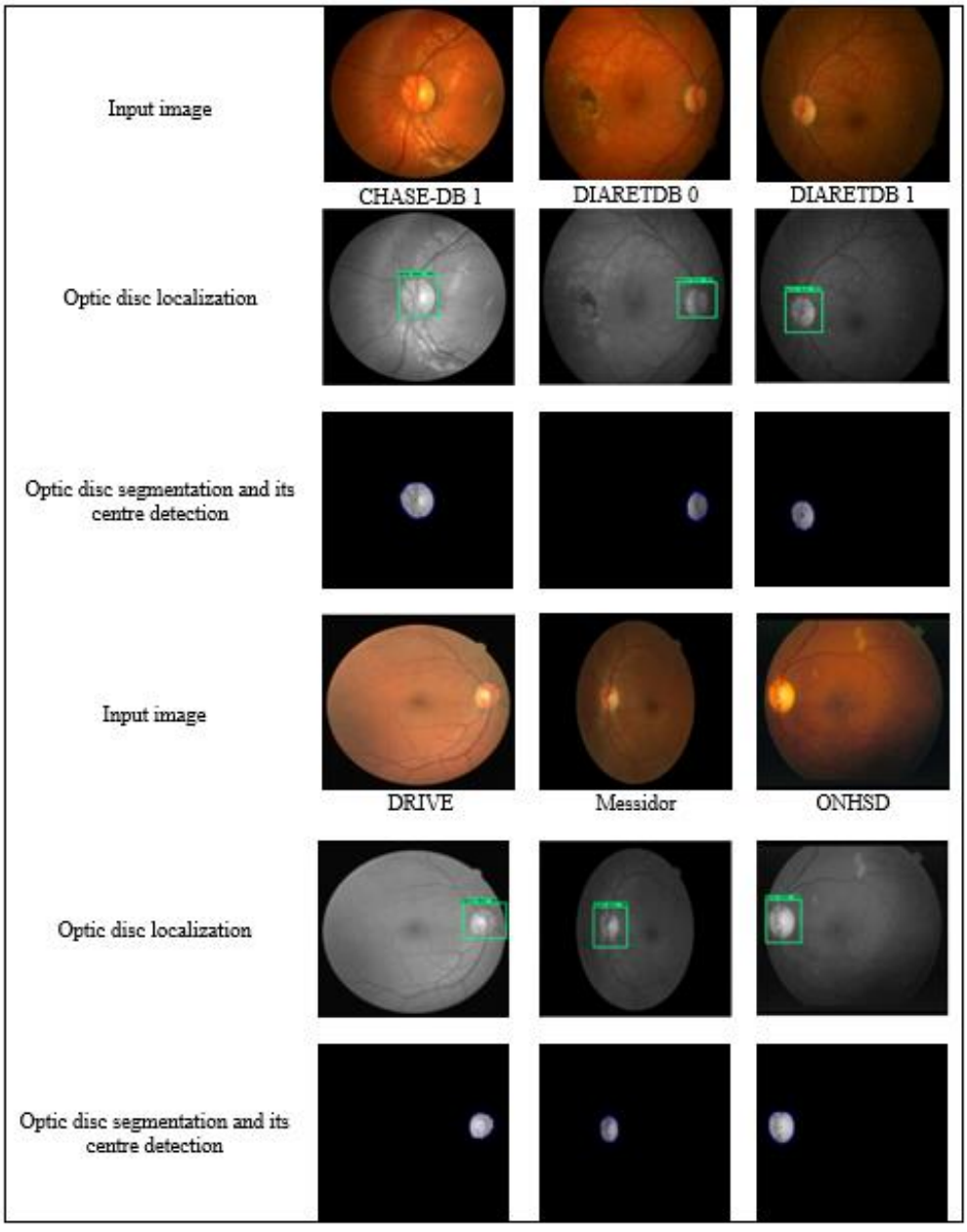

Figure 11. Optic disc segmentation in public databases

Figure 12 shows the cases where the precise segmentation of optic disc has failed. This is mainly due to the uneven distribution of pixels in the OD region which the GarbCut algorithm was unable to segment as the foreground object accurately.

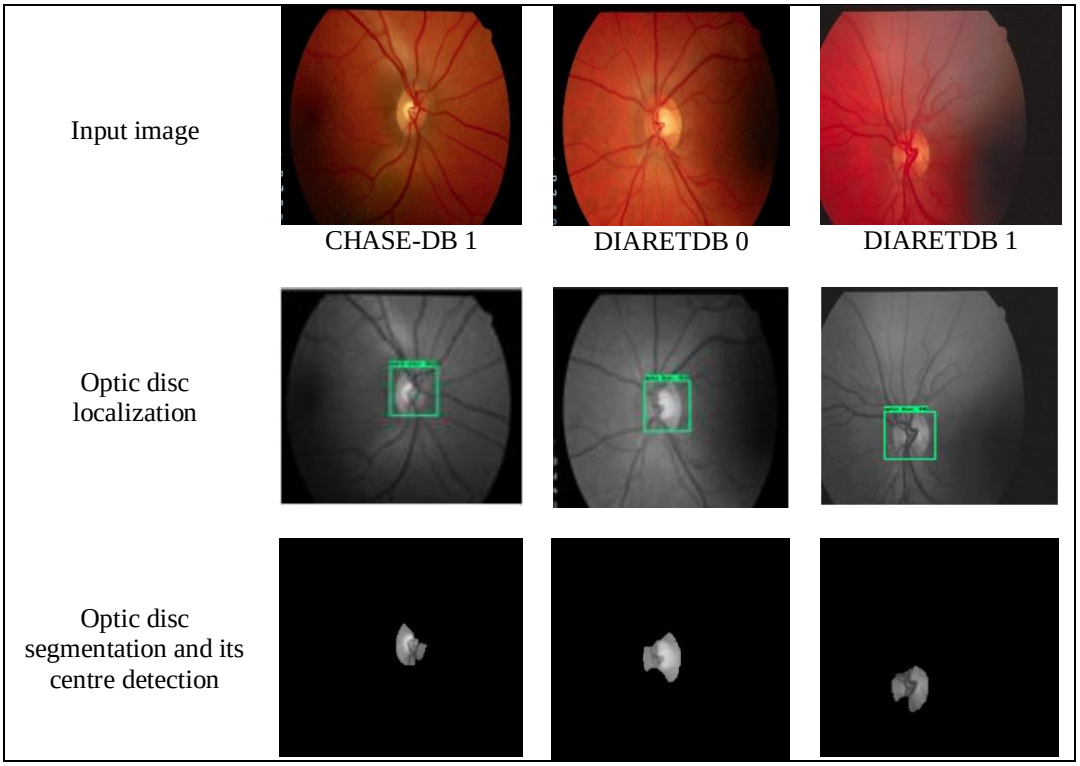

Figure 12. Failure in precise optic disc segmentation

5. CONCLUSION

The proposed method locates and segments the optic disc with higher accuracy and finds its diameter irrelevant of its position and its orientation in the retinal images. The usage of image quality assessment network helps in discarding the retinal images of bad quality and hence focuses only on the good quality images. The efficiency of Inception v-3 network to define the ROI in combination with the GrabCut algorithm for object segmentation is exploited for the first time to precisely segment the optic disc in color fundus images. The proposed method outperforms several existing methods for fundus IQA and OD segmentation.

ACKNOWLEDGEMENTS

We sincerely thank Kasturba Medical College (KMC), Manipal, India, for providing the required fundus images for our experimentation. We also thank Manipal Academy of Higher Education (MAHE) for the financial support and the resources provided during our research work. Our sincere thanks to the Department of Computer Science & Engineering, Manipal Institute of Technology, Manipal, India, for the guidance and technical support provided.

REFERENCES

[1] Y. C. Tham, *et al.*, "Global prevalence of glaucoma and projections of glaucoma burden through 2040: A systematic review and meta-analysis,:" *Ophthalmology*, vol. 121(11), pp. 2081-2090, 2014.
[2] A. Almazroa, *et al.*, "Optic disc and optic cup segmentation methodologies for glaucoma image detection: A survey," *J. Ophthalmology*, 2015.
[3] H. A. Quigley and A. T. Broman, "The number of people with glaucoma worldwide in 2010 and 2020," *British J. Ophthalmology*, vol. 90(3), pp. 262–267, 2006.
[4] Thylefors B, *et al.*, "Global data on blindness," *Bull World Health Organization*, vol. 73(1), pp. 115-21, 1995.

[5] Arpit Bansal, *et al.*, "An efficient automatic intensity based method for detection of Macula in retinal images," *38th IEEE International Conference on Telecommunications and Signal Processing (TSP-2015)*, Prague, Europe, *IEEE Xplore Digital Library*, 2015.
[6] U. Raghavendra, *et al.*,"Deep convolution neural network for accurate diagnosis of glaucoma using digital fundus images," *Information Sciences*, vol. 441, pp. 41-49, 2018.
[7] Li H., Chutatape O., "Automated feature extraction in color retinal images by a model based approach," *IEEE Transactions on Biomed. Engineering*, vol. 51, pp. 246-254, 2004.
[8] Li Xiong, Huiqi Li., "An approach to locate optic disc in retinal images with pathological changes," *Computerized Medical Imaging and Graphics*, 2016.
[9] Sajib Kumar Saha, *et al.*, "Automated quality assessment of colour fundus images for diabetic retinopathy screening in telemedicine," *Journal of Digital Imaging*, vol. 31(6), pp. 869-878, 2018.
[10] Aaron S. Coyner *et al.*, "Deep learning for image quality assessment of fundus images in retinopathy of prematurity," *AMIA Annu. Symp. Proc*., pp. 1224-1232, 2018.
[11] X. Xia, *et al.*, "Inception-v3 for flower classification," *2nd International Conference on Image*, pp. 783-787, 2017.
[12] C. Rother, *et al.*, "GrabCut: Interactive foreground extraction using iterated graph cuts," *ACM Transactions on Graphics*, vol. 23(3), pp. 309-314, 2004.
[13] Mahapatra, *et al.*, "A cnn based neurobiology inspired approach for retinal image quality assessment," *IEEE 38th Annual Int. Conf. of the Engineering in Medicine and Biology Society (EMBC)*, Orlando, USA, pp. 1304-1307, 2016.
[14] Yu, F., Sun, J., Li, A., *et al.*, "Image quality classification for dr screening using deep learning," *39th Annual Int. Conf. of the IEEE Engineering in Medicine and Biology Society (EMBC)*, Seogwipo, South Korea, pp. 664-667, 2017.
[15] Achanta, R., *et al.*, "“Frequency-tuned salient region detection," *IEEE Conf. on computer vision and pattern recognition, CVPR 2009*, Miami Beach, USA, pp. 1597-1604, 2009.
[16] K.-K. Maninis, *et al.*, "Deep retinal image understanding," in *Proc. Int. Conf. on Medical Image Computing and Computer-Assisted Intervention, Springer*, pp. 140-148, 2016.
[17] A. Sevastopolsky, "Optic disc and cup segmentation methods for glaucoma detection with modification of u-net convolutional neural network," *Pattern Recognition and Image Analysis*, vol. 27(3), pp. 618-624, 2017.
[18] Huazhu Fu, *et al.*, "Joint optic disc and cup segmentation based on multi-label deep network and polar transformation," *IEEE transactions on medical imaging*, vol. 37(7), 2018.
[19] C. Rother, *et al.*, "GrabCut: Interactive foreground extraction using iterated graph cuts," *ACM Transactions on Graphics*, vol. 23(3), pp. 309-314, 2004.
[20] Boykov, Y and Jolly, M., "Interactive graph cuts for optimal boundary and region segmentation of objects in N-D images," *In Proc. IEEE Int. Conf. on Computer Vision*, CD-ROM, 2001.
[21] M.B. Salah, *et al.*, "Multiregion image segmentation by parametric kernel graph cuts," *IEEE Trans. Image Process*.,vol. 20(2), pp. 545-557, 2011.
[22] Yi Lai, *et al.*, "Image segmentation via grabcut and linear multi-scale smoothing," *Proceedings of the 3rd International Conference on Communication and Information Processing*, 2017.
[23] Lan-Rong Dung, *et al.*, "A hierarchical grab cut image segmentation algorithm," *Journal of Computer and Communications*, vol. 6, pp. 48-55, 2018.
[24] Ioffe Sergey and Szegedy Christian, "Batch normalization: Accelerating deep network training by reducing internal covariate shift," *arXiv preprint arXiv:1502.03167*, 2015.
[25] Nitish Srivastava, *et al.*, "Dropout: A simple way to prevent neural networks from overfitting," *The Journal of machine learning research*, vol. 15(1), pp. 1929-1958, 2014.
[26] L. B. Lucy, "An iterative method for the rectification of observed distributions," *Astronomical J.*, vol. 79, pp. 745-754, (1974).
[27] W. H. Richardson, "Bayesian-based iterative method of image restoration," *J. Opt. Soc. Am.*, vol. 62, pp. 55-59, 1972.
[28] K. Zuiderveld, *Contrast limited adaptive histogram equalization*, Academic Press Inc., 1994.
[29] A. Reza, "Realization of the Contrast Limited Adaptive Histogram Equalization (CLAHE) for real-time image enhancement," *Journal of VLSI Signal Processing*, vol. 38, pp. 35-44, 2004.
[30] Justin F. Talbot and Xiaoqian Xu, "Implementing GrabCut," *Brigham Young University*, Revised: Apr 2006.
[31] Hamers L, *et al.*, "Similarity measures in scientometric research: The jaccard index versus salton's cosine formula," *Inf. Process. Manage*, pp 315-318, 1989.
[32] Aquino, A. *et al.*, "Detecting the optic disc boundary in digital fundus images using morphological edge detection and feature extraction techniques," *IEEE Trans. Med. Imaging*, vol. 20 (11), pp. 1860-1869, 2010.
[33] Cheng, J., Liu, J., *et al.*, "Superpixel classification based optic disc and optic cup segmentation for glaucoma screening," *IEEE Trans. Med. Imaging*, vol. 32(6), pp. 1019-1032, 2013.
[34] Joshi, G.D., *et al.*, "Optic disk and cup segmentation from monocular color retinal images for glaucoma assessment," *IEEE Trans. Med. Imaging*, vol. 30(6), pp. 1192-1205, 2011.
[35] Julian Zilly, *et al.*, "Glaucoma detection using entropy sampling and ensemble learning for automatic optic cup and disc segmentation," *Computerized Medical Imaging and Graphics*, vol. 55, pp. 28-41, 2017.

BIOGRAPHIES OF AUTHORS

Bhargav Bhatkalkar is currently working as an Assistant Professor-Senior scale in the Department of Computer Science & Engineering at MIT, Manipal, India. He is pursuing Ph.D. from MIT, Manipal Academy of Higher Education, Manipal in the area of medical image analysis using machine learning techniques. He has more than 13 years of teaching experience and industry experience. His areas of research interests are Image Processing, Pattern recognition, Medical image analysis, Machine learning and Data security.

Abhishek Joshi is currently pursuing his bachelor's degree in Electronics & Communication Engineering at MIT, Manipal. His areas of research interest are Image processing, Robotics, and Human-Computer Interaction.

Dr. Srikanth Prabhu is currently working as Associate Professor in the Department of Computer Science & Engineering at MIT, Manipal, India. He completed his Ph.D. from IIT Kharagpur. He has more than 20 years of teaching experience. His areas of research interests are Image processing, Pattern recognition, Parallel processing, and Artificial intelligent.

Dr. Sulatha Bhandary is Professor & Head of Ophthalmology Department, KMC, Manipal. She has more than 17 years of working experience. Her research interests are Cataract diagnosis and treatment, Retinal imaging.